

# Accelerated dystrophy and decay of oligodendrocyte precursor cells in the APP/PS1 model of Alzheimer's-like pathology

Irene Chacon-De-La-Rocha<sup>1</sup>, Gemma Fryatt<sup>2</sup>, Andrea D. Rivera<sup>1</sup>, Alexei Verkhratsky<sup>3</sup>, Olivier Raineteau<sup>4</sup>, Diego Gomez-Nicola<sup>2</sup>, Arthur M. Butt<sup>1\*</sup>

<sup>1</sup>University of Portsmouth, United Kingdom, <sup>2</sup>University of Southampton, United Kingdom, <sup>3</sup>Manchester University, United States, <sup>4</sup>Université Claude Bernard Lyon 1, France

*Submitted to Journal:*  
Frontiers in Cellular Neuroscience

*Specialty Section:*  
Non-Neuronal Cells

*Article type:*  
Original Research Article

*Manuscript ID:*  
575082

*Received on:*  
22 Jun 2020

*Revised on:*  
21 Oct 2020

*Frontiers website link:*  
[www.frontiersin.org](http://www.frontiersin.org)

---

### *Conflict of interest statement*

The authors declare a potential conflict of interest and state it below

AMB and ADR declare they are share-holders and co-founders of the company GliaGenesis Ltd. All the authors declare that they have no other competing interests.

### *Author contribution statement*

IC-D-L-R: Formal Analysis; Investigation; Methodology; Writing - original draft.

GF: Formal Analysis; Investigation; Methodology; Validation.

ADR: Investigation.

AV: Conceptualization; Writing - review & editing.

OR: Resources; Writing - review & Editing

DG-N: Conceptualization; Data curation; Formal analysis; Funding acquisition; Project administration; Resources; Supervision; Validation; Visualization; Writing - review & editing.

AMB: Conceptualization; Data curation; Formal analysis; Funding acquisition; Project administration; Resources; Supervision; Validation; Visualization; Writing - original draft; Writing - review & editing.

### *Keywords*

Hippocampus, myelin, OPC, Oligodendrocyte progenitor cell, Alzheimer's disease

### *Abstract*

Word count: 175

Myelin disruption is a feature of natural aging and of Alzheimer's disease (AD). In the CNS, myelin is produced by oligodendrocytes, which are generated throughout life by oligodendrocyte progenitor cells (OPCs). Here, we examined age-related changes in OPCs in APP/PS1 mice, a model for AD-like pathology, compared with non-transgenic (Tg) age-matched controls. Analysis was performed in the CA1 area of the hippocampus following immunolabelling for NG2 with the nuclear dye Hoescht, to identify OPC and OPC sister cells, a measure of OPC replication. The results indicate a significant decrease in the number of OPCs at 9 months in APP/PS1 mice, compared to age-matched controls, without further decline at 14 months. In addition, the number of OPC sister cells declined significantly at 14-months in APP/PS1 mice, which was not observed in age-matched controls. Notably, OPCs also displayed marked morphological changes at 14 months in APP/PS1 mice, characterized by an overall shrinkage of OPC process domains and increased process branching. The results indicate that OPC disruption is a pathological sign in the APP/PS1 mouse model of AD.

### *Contribution to the field*

There is increasing recognition that glial cells are important in the pathogenesis of Alzheimer's disease (AD). In recent years, evidence has accumulated that myelin loss occurs at an early stage of AD, but the reasons are unknown. In this study, we describe age-dependent changes in oligodendrocyte progenitor cells (OPC) in the APP/PS1 mouse model of AD. Our results demonstrate that OPC disruption is a pathological sign in this mouse model and is a potential factor in accelerated myelin loss and cognitive decline.

### *Funding statement*

Supported by grants from the BBSRC (AB, AR, Grant Number BB/M029379/1), MRC (AB, Grant Number MR/P025811/1), Alzheimer's Research UK (DG, AB, Grant Number ARUK-PPG2014B-2), University of Portsmouth PhD Programme (AB, ICR), and a grant from the "Programme Avenir Lyon Saint-Etienne" (OR).

Open Access publication fees paid by University of Portsmouth.

### *Ethics statements*

#### *Studies involving animal subjects*

Generated Statement: The animal study was reviewed and approved by All animal procedures were carried out in accordance with the Animals (Scientific Procedures) Act 1986 of the UK..

#### *Studies involving human subjects*

Generated Statement: No human studies are presented in this manuscript.

#### *Inclusion of identifiable human data*

Generated Statement: No potentially identifiable human images or data is presented in this study.

In review

### *Data availability statement*

Generated Statement: The datasets presented in this article are not readily available because No datasets were generated in this study. All data generated or analysed during this study are included in this published article.. Requests to access the datasets should be directed to [arthur.butt@port.ac.uk](mailto:arthur.butt@port.ac.uk).

In review

# Accelerated dystrophy and decay of oligodendrocyte precursor cells in the APP/PS1 model of Alzheimer's-like pathology

1 †Irene Chacon-De-La-Rocha<sup>1</sup>, †Gemma Fryatt<sup>2</sup>, Andrea Rivera<sup>1</sup>, Alex Verkhratsky<sup>3</sup>, Olivier  
2 Raineteau<sup>4</sup>, Diego Gomez-Nicola<sup>2\*</sup>, Arthur M. Butt<sup>1\*</sup>

3 <sup>1</sup>Institute of Biomedical and Biomolecular Sciences, School of Pharmacy and Biomedical Sciences,  
4 University of Portsmouth, UK.

5 <sup>2</sup>School of Biological Sciences, Southampton General Hospital, University of Southampton, UK.

6 <sup>3</sup>Faculty of Biology, Medicine and Health, University of Manchester, UK.

7 <sup>4</sup>Univ Lyon, Université Claude Bernard Lyon 1, Inserm, Stem Cell and Brain Research Institute  
8 U1208, 69500 Bron, France.

9  
10 †Authors contributed equally to the paper.

11 \*Corresponding authors: Arthur M. Butt, Email: [arthur.butt@port.ac.uk](mailto:arthur.butt@port.ac.uk); Diego Gomez-Nicola  
12 [d.gomez-nicola@soton.ac.uk](mailto:d.gomez-nicola@soton.ac.uk)

13

14 Keywords: oligodendrocyte progenitor cell, OPC, myelin, hippocampus, Alzheimer's disease

15

## 16 Abstract

17 Myelin disruption is a feature of natural aging and of Alzheimer's disease (AD). In the CNS, myelin  
18 is produced by oligodendrocytes, which are generated throughout life by oligodendrocyte progenitor  
19 cells (OPCs). Here, we examined age-related changes in OPCs in APP/PS1 mice, a model for AD-like  
20 pathology, compared with non-transgenic (Tg) age-matched controls. Analysis was performed in the  
21 CA1 area of the hippocampus following immunolabelling for NG2 with the nuclear dye Hoescht, to  
22 identify OPC and OPC sister cells, a measure of OPC replication. The results indicate a significant

23 decrease in the number of OPCs at 9 months in APP/PS1 mice, compared to age-matched controls,  
 24 without further decline at 14 months. In addition, the number of OPC sister cells declined significantly  
 25 at 14-months in APP/PS1 mice, which was not observed in age-matched controls. Notably, OPCs also  
 26 displayed marked morphological changes at 14 months in APP/PS1 mice, characterized by an overall  
 27 shrinkage of OPC process domains and increased process branching. The results indicate that OPC  
 28 disruption is a pathological sign in the APP/PS1 mouse model of AD.

29

### 30 **Introduction**

31 Alzheimer's disease (AD) is the most common type of dementia and it is characterized by the formation  
 32 of intracellular neurofibrillary tangles (NFTs) and extracellular amyloid- $\beta$  (A $\beta$ ) plaques (Braak and  
 33 Braak, 1991). White matter disruption is present at an early stage of AD pathology (Bartzokis, 2011,  
 34 Ihara et al., 2010), and post-mortem analyses indicate that a loss of oligodendrocytes in AD could serve  
 35 as a diagnostic tool for differentiating white matter pathologies in dementia (Sjöbeck and Englund,  
 36 2003, Brickman et al., 2015). Studies in human AD and mouse models indicate loss of  
 37 oligodendrocytes and demyelination is most pronounced at the core of A $\beta$  plaques (Mitew et al., 2010).  
 38 Hence, myelin loss is a feature of human AD and mouse models (Desai et al., 2009), but the underlying  
 39 causes are unresolved.

40

41 In the adult brain, oligodendrocyte progenitor cells (OPCs) are responsible for the life-long generation  
 42 of oligodendrocytes, required to myelinate new connections formed in response to new life  
 43 experiences, and to replace myelin lost in pathology (Xiao et al., 2016, McKenzie et al., 2014, Young  
 44 et al., 2013, Hughes et al., 2018). OPCs are identified by their expression of the NG2 proteoglycan and  
 45 are sometimes known as NG2-cells or NG2-glia (Butt et al., 2002). Prior to differentiating into mature  
 46 myelinating oligodendrocytes, OPCs transition through an intermediate phase identified by expression

47 of the G-protein coupled receptor GPR17 (Viganò et al., 2016). Notably, early changes in OPCs may  
48 be a pathological sign and underlie myelin loss in mouse models of AD-like pathology (Rivera et al.,  
49 2016, Mitew et al., 2010, Vanzulli et al., 2020). This possibility is supported by immunostaining of  
50 post-mortem AD brain showing reduced NG2 immunoreactivity in individuals with high A $\beta$  plaque  
51 load (Nielsen et al., 2013b).

52

53 The APP/PS1 transgenic mouse expresses familial AD-causing mutated forms of human APP  
54 (APP<sup>swe</sup>, Swedish familial AD-causing mutation) and presenilin1 (PS1<sup>dE9</sup>) and is used extensively  
55 as a model for AD-like pathology (Borchelt et al., 1997). The APP/PS1 mouse presents early A $\beta$  plaque  
56 deposition in the hippocampus at 4-5 months of age and extensively throughout the forebrain by 8  
57 months (Borchelt et al., 1997), which is linked to greatly impaired synaptic long-term potentiation  
58 (LTP) after 8 months of age in the CA1 area of the hippocampus in APP/PS1 (Gengler et al., 2010).  
59 Furthermore, several studies provide evidence that white matter and myelin disruption are early clinical  
60 signs of APP/PS1 mice (Dong et al., 2018, Wu et al., 2017, Shu et al., 2013, Chao et al., 2018), with  
61 evidence that myelin disruption in APP/PS1 mice aged 6 months is accompanied by decreased learning  
62 and spatial behavior performance (Dong et al., 2018, Chao et al., 2018). In addition, there is evidence  
63 of increased NG2 cell numbers in the temporal lobe of 6 months old APP/PS1 mice (Dong et al., 2018),  
64 and clustering of hypertrophic NG2 cells around A $\beta$  plaques in the cortex of 14 month old APP/PS1  
65 (Li et al., 2013). Here, we examined changes in OPCs in 9 and 14 months old APP/PS1 mice, compared  
66 to age-matched non-transgenic controls, and focused on the AD-relevant CA1 area of the hippocampus.  
67 Our results indicate a premature decline in OPC numbers at 9 months in APP/PS1, whilst at 14 months  
68 OPCs displayed cellular shrinkage and increased process branching in APP/PS1, characteristic of  
69 reactive changes in response to pathology (Ong and Levine, 1999, Butt et al., 2002). This study  
70 identifies pathological changes in OPCs in the APP/PS1 mouse model of AD.

71

72 **MATERIAL AND METHODS**73 *Ethics*

74 The animal study was reviewed and approved by the University of Southampton Animal Welfare  
75 Ethical Review Body (AWERB). All procedures were carried out in accordance with the Animals  
76 (Scientific Procedures) Act 1986 of the UK.

77

78 *Animals and tissue*

79 Transgenic APP/PS1 mice were used that contain human transgenes for both APP (KM670/671NL,  
80 Swedish) and PSEN1 (L166P). APP<sup>swe</sup>/PSEN1<sup>dE9</sup> mice (APP/PS1) on a C57BL/6 background were  
81 originally obtained from the Jackson Laboratory and heterozygous males were bred at our local  
82 facilities with wild-type female C57BL/6J (Harlan). Offspring were ear punched and genotyped using  
83 PCR with primers specific for the APP-sequence (forward: GAATTCGACATGA CTCAGG,  
84 reverse: GTTCTGCTGCATCTTGGACA). Mice not expressing the transgene were used as non-  
85 transgenic wild-type littermate controls. Mice were housed in groups of 4 to 10, under a 12-h light/12h  
86 dark cycle at 21°C, with food and water ad libitum. No mice were excluded and experimental groups  
87 contained a spread of sexes. Mice weight was monitored throughout the experiment. APP/PS1 mice  
88 and age matched non-transgenic controls aged 9 and 14 months old were perfusion fixed intracardially  
89 under terminal anaesthesia with 4% paraformaldehyde (PFA), then post-fixed for 2 hours with 4%  
90 PFA. Sections were cut on a vibratome (Leica) at a thickness of 35 µm then stored in cryoprotectant at  
91 -70°C until use.

92

93 *Immunohistochemistry*

94 Sections were treated for a blocking stage of either 10-20% normal goat serum (NGS) or normal  
95 donkey serum (NDS) or 0.5% bovine serum albumin (BSA) for 1-2 h, depending on the primary  
96 antibodies to be used. Sections were washed 3 times in PBS, and incubated overnight in primary  
97 antibody diluted in blocking solution containing 0.25% Triton-X: rabbit anti-NG2, 1:500 (Millipore);  
98 rabbit anti-Olig2, 1:500 (Millipore); rabbit anti-GPR17, 1:100 (Cayman Labs); rat anti-MBP, 1:300  
99 (Millipore). Sections were washed 3 times in PBS, and incubated overnight in primary antibody diluted  
100 in blocking solution containing 0.25% Triton-X: rabbit anti-NG2, 1:500 (Millipore); rabbit anti-Olig2,  
101 1:500 (Millipore); rabbit anti-GPR17, 1:100 (Cayman Labs); rat anti-MBP, 1:300 (Millipore). Tissues  
102 were then washed 3 times in PBS and incubated with appropriate fluorochrome secondary antibody  
103 (AlexaFluor® 488, AlexaFluor® 568, 1:400, Life Technologies), or biotinylated secondary antibody  
104 (Vector Labs) diluted in blocking solution for 1-2h. Finally, sections were washed 3 times with PBS  
105 before being mounted on glass slides and covered with mounting medium and glass coverslips ready  
106 for imaging.

107

108 *Imaging and Analysis*

109 Immunofluorescence images were captured using a Zeiss Axiovert LSM 710 VIS40S confocal  
110 microscope and maintaining the acquisition parameters constant to allow comparison between samples  
111 within the same experiment. Acquisition of images for cell counts was done with x20 objective. Images  
112 for OPC reconstruction were taken using x100 objective and capturing z-stacks formed by 80-100  
113 single plains with an interval of 0.3  $\mu\text{m}$ . Cell counts were performed in the CA1 area in projected  
114 flattened images from z-stacks formed by 10 or 15 z-single plain images with 1 $\mu\text{m}$  interval between  
115 them, and cell density was calculated as the total number of cells per unit area expressed as cells per  
116  $\text{mm}^2$ . The relative density of MBP immunolabelling was measured within a constant field of view  
117 (FOV) using ImageJ. For DAB immunostaining of Olig2+ oligodendrocytes, sections were examined

118 on an Olympus dotSlide digital slide scanning system based on a BX51 microscope stand with  
119 integrated scanning stage and Olympus CC12 colour camera. The cell coverage of OPCs was measured  
120 using ImageJ by drawing a line around the cell processes and measuring the area enclosed within the  
121 line and expressing the data relative to the area of the CA1 in each section. For morphological analysis  
122 of single OPCs, cells were drawn using NeuroLucida 360 and their morphology was analysed using  
123 NeuroLucida 360 explorer for measurements of the number of processes per cell, number of process  
124 terminals (end-points), number of nodes (branch points) and cell complexity; OPC cell complexity  
125 refers to the normalization and comparison of processes derived from the dendritic complexity index  
126 described (Pillai et al., 2012), whereby NeuroLucida 360 Explorer calculated cell *complexity* from the  
127 sum of [*terminal orders* + *number of terminals*] multiplied by the [*total dendritic length* / *number of*  
128 *primary dendrites*], where *terminal* is defined as a process ending and *terminal order* is the number of  
129 branches along a process, between the cell body and the terminal (calculated for each terminal). For  
130 Sholl analysis, the interval between Sholl shells was 5µm. Data were expressed as Mean±SEM and  
131 tested for significance by ANOVA followed by Tukey's post-hoc test for cell numbers, myelin  
132 immunostaining, OPC cell domains and neuroLucida analyses of OPCs, and Sidak's multiple  
133 comparisons test for Sholl analysis, using GraphPad Prism 6.0.

134

## 135 **RESULTS**

### 136 ***Premature decline of OPCs in the hippocampus of APP/PS1 mice***

137 The hippocampus displays a high degree of adult oligodendrogenesis, which is important for learning  
138 and plasticity (Steadman et al., 2020). Here, we used NG2 immunolabelling to identify adult OPCs  
139 (Nishiyama et al., 2016) in the CA1 area of the hippocampus (Fig. 1); NG2 is also expressed by  
140 pericytes, which are directly applied to blood vessels and readily distinguished from OPCs, which are  
141 distinguished by their complex process bearing morphology (Hamilton et al., 2010). OPCs are

142 uniformly distributed throughout the hippocampus at both 9 and 14 months, in APP/PS1 mice and age-  
143 matched controls (Fig. 1A, B). NG2<sup>+</sup> OPCs are often observed as duplets or triplets (some indicated  
144 by arrows in Fig. 1A, B, and at higher magnification in the inset in Fig. 1A). OPC duplets have been  
145 shown to be recently divided sister cells and their frequency is a measure of OPC cell division (Boda  
146 et al., 2014), confirming previous studies that adult OPCs continue to divide slowly in old age (Young  
147 et al., 2013, Psachoulia et al., 2009). Quantification confirmed a significant difference in the numerical  
148 density of NG2<sup>+</sup> OPCs in APP/PS1 at 9 months compared to age-matched controls (Fig. 1C; two-way  
149 ANOVA  $p \leq 0.05$ , followed by Tukey's post hoc test). The data indicated a 50% decrease in NG2<sup>+</sup>  
150 OPCs at 9 months in APP/PS1 to a level observed at 14 months in natural ageing (Fig. 1C); there was  
151 no further decline in OPC numbers between 9 and 14 months APP/PS1 mice, which were the same as  
152 age-matched controls (Fig. 1C). In addition, there was a significant decrease in the numerical density  
153 of OPC sister cells at 14 months in APP/PS1 mice (Fig. 1D; two-way ANOVA  $p \leq 0.05$ , followed by  
154 Tukey's post hoc test,  $p \leq 0.05$ ). Overall, the results indicate a premature decline in OPC numbers at 9  
155 months in APP/PS1 mice.

156

### 157 *Decline in myelination in the hippocampus of APP/PS1 mice*

158 The hippocampus displays a high degree of myelination, which is essential for cognitive function  
159 (Abraham et al., 2010), and myelination has been shown to be disrupted in this area in APP/PS1 mice  
160 and it is relevant to AD pathology (Ota et al., 2019, Chao et al., 2018, Dong et al., 2018).  
161 Immunolabelling for MBP is prominent in the CA1 area at both 9- and 14-months in controls and in  
162 APP/PS1 (Fig. 2A, B), as are GPR17<sup>+</sup> cells, which are an intermediate stage between OPCs and  
163 myelinating oligodendrocytes (upper insets, Fig. 2A, B), and Olig2<sup>+</sup> cells, which is expressed by all  
164 oligodendroglial cells (lower insets, Fig. 2A, B). Between 9- and 14- months of age, we observed no  
165 significant changes in the numerical density of GPR17<sup>+</sup> and Olig2<sup>+</sup> oligodendrocytes in controls or

166 APP/PS1 (Fig. 2C, D), and so we did not analyse oligodendrocyte cell numbers further; it should be  
167 noted there was wide variability in GPR17+ cells at 14-months in controls, but overall there was  
168 difference in the number of GPR17+ cells in APP/PS1 between 9- and 14-months in the CA1 region  
169 of the hippocampus. Significant age-related changes in MBP immunostaining were detected in the  
170 CA1 region and this was not observed in APP/PS1 mice (Fig. 2E; ANOVA,  $p \leq 0.01$ , followed by  
171 Tukey's post hoc tests). Overall, the results indicate MBP immunostaining is retarded at later stages of  
172 pathology in APP/PS1 mice.

173

#### 174 ***OPC exhibit cellular shrinkage at 14 months in APP/PS1 mice***

175 The results above indicate OPC are disrupted in APP/PS1 mice, which is often associated with changes  
176 in OPC morphology in AD and other pathologies (Butt et al., 2019a, Butt et al., 2019b, Vanzulli et al.,  
177 2020). We therefore examined OPC morphology in depth, using high magnification confocal images  
178 and measuring the process domains of individual cells and the total coverage of NG2 cells within the  
179 CA1 (Fig. 3). Significant differences were detected in the size of OPC process domains in 14 month  
180 APP/PS1 (Fig. 3Biii; ANOVA,  $p \leq 0.001$ , followed by Tukey's post hoc test,  $p \leq 0.001$ ); no differences  
181 were observed in OPCs at 9-months in APP/PS1 compared to controls. The results indicate that at 14-  
182 months OPCs display a significant shrinkage in APP/PS1.

183

#### 184 ***OPC exhibit increased process branching and cellular complexity at 14 months in APP/PS1 mice***

185 The underlying morphological changes resulting in OPC shrinkage in APP/PS1 mice were examined  
186 in further detail using NeuroLucida cell tracing. Confocal images of 80-100 z-sections, each of 0.3 $\mu$ m  
187 thickness, were captured using a x100 oil objective and reconstructed and analyzed using NeuroLucida  
188 360 and NeuroLucida 360 Explorer (Fig. 4A, B;  $n=9$  cells from 3 animals in each group). Consistent  
189 with the results above, OPC morphology was significantly altered at 14-months in APP/PS1 compared

190 to age-matched controls, with the average number of processes per cell being unaltered (Fig. 4C),  
191 whereas processes displayed increased branching, with a significantly greater number of process  
192 terminals or end points (Fig. 4D; ANOVA  $p \leq 0.01$ , followed by Tukey's post hoc test,  $p \leq 0.05$ ) and  
193 number of branch points or nodes (Fig. 4E; ANOVA  $p \leq 0.01$ , followed by Tukey's post hoc test,  
194  $p \leq 0.01$ ), with a consequent 3-fold increase in the NeuroLucida measurement of cell complexity in 14-  
195 month APP/PS1 compared to age-match controls (Fig. 4F; ANOVA  $p \leq 0.01$ , followed by Tukeys post  
196 hoc test,  $p \leq 0.01$ ). In contrast, no changes in the morphological parameters of OPCs were detected  
197 between 9- and 14-months in wild-type mice (Fig. 4C-F) or in 9-month APP/PS1 OPC compared to  
198 age-matched controls (Fig. 4C-F). The age-related changes in OPC complexity in APP/PS1 mice was  
199 examined further using Sholl analysis (Fig. 5A;  $n=9$  cells for each group, ANOVA followed by Sidak's  
200 multiple comparisons test). Sholl analysis confirmed significant differences in OPC morphology in  
201 APP/PS1 mice between 9 and 14 months, with significant increases in the number of end points (Fig.  
202 5B), the number of nodes (Fig. 5C), and in process lengths (Fig. 5D). In addition, analysis of processes  
203 length in the different branch orders identified that OPCs displayed increased process length in the  
204 distal branches (Fig. 5E). In contrast to these changes in APP/PS1, no significant differences were  
205 found in OPC morphology in natural aging (Fig. 5, insets); at 14 months, OPCs displayed a decrease  
206 in process lengths in the proximal branches, whereas this parameter was increased in APP/PS1 at 14  
207 months (Fig. 5E, inset). It is important to note that the small number of cells analysed by NeuroLucida  
208 and Sholl may have introduced the possibility of bias. Nonetheless, the measurements of OPC process  
209 domains, together with NeuroLucida and Sholl analyses, all indicate that OPC shrinkage is a key feature  
210 in APP/PS1 at 14-months and is associated with increased process branching, giving OPCs a more  
211 fibrous appearance that is similar to 'reactive' NG2 cells reported in human AD and AD models (Li et  
212 al., 2013, Nielsen et al., 2013a, Vanzulli et al., 2020), as well as injury models (Jin et al., 2018, Butt et  
213 al., 2005, Ong and Levine, 1999), and this was not observed in age-matched controls

214 **Discussion**

215 Age-related loss of myelin has been shown to be a pathological feature of human AD (Bartzokis, 2011,  
216 Brickman et al., 2015) and in animal models of AD (Dong et al., 2018, Desai et al., 2009, Mitew et al.,  
217 2010, Vanzulli et al., 2020). We observed a decrease in MBP immunostaining at 14 months in the  
218 hippocampus of APP/PS1 mice, consistent with evidence that myelination is disrupted in this model  
219 of AD (Dong et al., 2018, Wu et al., 2017, Shu et al., 2013, Chao et al., 2018). The key findings of the  
220 present study are that there is a premature decrease in OPC density at 9-months in APP/PS1 mice, and  
221 that at 14-months OPC displayed a shrunken and fibrous morphology, indicative of morphological  
222 dystrophy. These findings indicate that changes in OPCs are potential factors in the progression of AD  
223 pathology.

224  
225 Our data support previous studies that there is a decline in the number of OPCs in natural ageing  
226 (Young et al., 2013). Notably, this age-related loss of OPCs occurred at 9 months of age in APP/PS1,  
227 indicating a premature loss of OPCs in this model of AD. The reduction in OPCs numbers at any point  
228 is a measure of changes in cell proliferation and/or death at earlier points, hence the reduction in OPC  
229 numbers at 9 months in APP/PS1 mice reflects an acceleration of the age-related loss of OPCs, which  
230 in natural aging occurs at later ages. The decrease in OPCs at 9 months in APP/PS1 indicates their  
231 capacity for self-renewal, defined as maintaining OPC numbers relatively constant over time, was  
232 reduced at a point prior to this age, which is consistent with evidence of advanced OPC senescence in  
233 7.5-month-old APP/PS1 mice (Zhang et al., 2019). We observed a reduction in OPC sister cells at 14  
234 months in APP/PS1, which is a measure of recently divided OPCs (Boda et al., 2014), suggesting that  
235 OPC self-renewal may be compromised at later ages in APP/PS1, although further studies are required  
236 to confirm this, for example using multiple injections of BrdU. The changes in OPCs were associated  
237 with a reduction in MBP immunostaining at 14-months in APP/PS1 mice compared to controls. MBP

238 immunostaining, taken as a measure of the overall extent of myelination, was increased between 9-  
239 and 14-months in wild-type controls, but not in APP/PS1 mice, consistent with multiple lines of  
240 evidence that myelination is disrupted in AD-like pathology (Dong et al., 2018, Wu et al., 2017, Shu  
241 et al., 2013, Chao et al., 2018, Desai et al., 2009, Mitew et al., 2010, Vanzulli et al., 2020). We did not  
242 detect evident changes in GPR17+ and Olig2+ oligodendrocytes, and no conclusions can be drawn on  
243 the overall numbers of oligodendrocytes at this time. The decrease in MBP immunostaining at 14-  
244 months in APP/PS1 mice may reflect changes in the number and lengths of myelin sheaths, which has  
245 been reported in aging (Hughes et al., 2018, Hill et al., 2018). Myelin remodelling is important for  
246 nervous system plasticity and repair (Ortiz et al., 2019, Chorghay et al., 2018, Williamson and Lyons,  
247 2018, Foster et al., 2019), and the decline in myelination in APP/PS1 may be related to neuronal loss  
248 and learning dysfunction in these mice (Chao et al., 2018). The results provide evidence of OPC and  
249 myelin disruption in the hippocampus of APP/PS1 mice, suggesting key features of human AD are  
250 replicated in this mouse model.

251

252 Notably, the early loss of OPCs at 9-months in APP/PS1 hippocampus is followed at 14-months by a  
253 more fibrous appearance of NG2+ OPCs due to cell shrinkage and increased branching, similar to the  
254 fibrous morphology of 'reactive' NG2-glia (Butt et al., 2002, Ong and Levine, 1999). Notably, fibrous  
255 or reactive NG2-glia have been reported to be associated with amyloid- $\beta$  plaques in human AD and  
256 mouse models (Nielsen et al., 2013b, Li et al., 2013, Vanzulli et al., 2020, Zhang et al., 2019), and  
257 further studies are required to determine whether OPC morphological changes depend on their relation  
258 to amyloid- $\beta$  plaques, as has been reported for astrocytes (Rodríguez et al., 2016). Since OPCs are the  
259 source of new myelinating oligodendrocytes in the adult brain (Rivers et al., 2008, Dimou et al., 2008,  
260 Zhu et al., 2008, Kang et al., 2010), it is possible their dystrophy in AD-like pathology may be a  
261 causative factor in myelin loss, but this will require comprehensive analyses to verify, such as fate-

262 mapping and live-cell imaging. Furthermore, the underlying causes of OPC shrinkage in APP/PS1 are  
 263 unresolved, but OPC are known to contact synapses in the hippocampus (Bergles et al., 2000), and  
 264 reduced synaptic activity is an important feature in APP/PS1 mice (Gengler et al., 2010), which could  
 265 result in retraction of OPC processes (Chacon-De-La-Rocha et al., 2020). In addition, neuronal activity  
 266 regulates myelination and myelin repair (Gibson et al., 2014, Wake et al., 2011, Ortiz et al., 2019), and  
 267 the observed disruption of OPCs suggests this may be an important factor in myelin loss in AD-like  
 268 pathology.

269

## 270 **Conclusions**

271 Our findings demonstrate that OPCs undergo complex age-related changes in the hippocampus of the  
 272 APP/PS1 mouse model of AD-like pathology. We conclude that OPC disruption is a pathological sign  
 273 in AD and is a potential factor in accelerated myelin loss and cognitive decline.

274

## 275 **Competing interests:**

276 AMB and ADR declare they are share-holders and co-founders of the company GliaGenesis Ltd. All  
 277 the authors declare that they have no other competing interests.

278

## 279 **Funding:**

280 Supported by grants from the BBSRC (AB, AR, Grant Number BB/M029379/1), MRC (AB, Grant  
 281 Number MR/P025811/1), Alzheimer’s Research UK (DG, AB, Grant Number ARUK-PPG2014B-2),  
 282 University of Portsmouth PhD Programme (AB, ICR), and a grant from the “Programme Avenir Lyon  
 283 Saint-Etienne” (OR)

284

## 285 **Authors' contributions:**

286 IC-D-L-R: Formal Analysis; Investigation; Methodology; Writing - original draft.

287 GF: Formal Analysis; Investigation; Methodology; Validation.

288 ADR: Investigation.

289 AV: Conceptualization; Writing - review & editing.

290 OR: Resources; Writing – review & Editing

291 DG-N: Conceptualization; Data curation; Formal analysis; Funding acquisition; Project  
292 administration; Resources; Supervision; Validation; Visualization; Writing - review & editing.

293 AMB: Conceptualization; Data curation; Formal analysis; Funding acquisition; Project  
294 administration; Resources; Supervision; Validation; Visualization; Writing - original draft; Writing -  
295 review & editing.

296

## 297 **Data Availability Statement**

298 All data generated or analysed during this study are included in this published article.

299

## 300 **Figure Legends**

301 **Figure 1 Changes in OPCs in the CA1 area of the hippocampus of APP/PS1 mice.** Hippocampi  
302 of 9months old and 14months old APP/PS1 mice were compared to age-matched controls. (A, B)  
303 Representative confocal images of immunofluorescence labelling for NG2 (green) to identify OPCs  
304 and counterstaining with Hoechst (blue) for nuclei, to identify OPC sister cells (some indicated by  
305 arrows), as illustrated at higher magnification (inset, Ai), from non-transgenic controls (Ai, Bi) and  
306 APP/PS1 mice (Aii, Bii), aged 9 months (Ai, Aii) and 14 months (Bi, Bii); scale bars = 50 $\mu$ m in main  
307 panels and 10  $\mu$ m in inset. (C, D) Bar graphs of the numerical density of NG2+ OPCs (C) and OPC  
308 sister cells (D). Data are expressed as Mean  $\pm$  SEM; \* $p$ <0.05, ANOVA followed by Tukey's post  
309 hoc test,  $n$ = 3 animals for each group.

310 **Figure 2 Changes in oligodendrocytes and myelin in the CA1 area of the hippocampus of**  
311 **APP/PS1 mice.** Hippocampi of 9months old and 14months old APP/PS1 mice were compared to  
312 age-matched controls. (A, B) Representative photomicrographs of immunolabelling for MBP (red) to  
313 identify the extent of myelination, together with GPR17 for immature oligodendrocytes (upper insets,  
314 green) and Olig2 for total number of oligodendrocyte lineage cells (lower panels, brown); scale bars =  
315 50 $\mu$ m, except upper insets = 20  $\mu$ m. (C-E) Bar graphs of numerical density of GPR17+ cells (C) and  
316 Olig2+ cells (D), together with MBP immunofluorescence density (E); data are expressed as Mean  $\pm$   
317 SEM; \* $p$ <0.05 ANOVA followed by Tukey's post hoc test,  $n$ = 3 animals for each group.

318 **Figure 3 OPC process domains in the CA1 area of the hippocampus of APP/PS1 mice.**  
319 Hippocampi of 9 months old and 14 months old APP/PS1 mice were examined, compared to age-  
320 matched controls, using immunofluorescence labelling for NG2 (green) to identify OPCs. High  
321 magnification confocal projections of OPCs and their process domains (indicated by broken white  
322 lines) in the 9 months old hippocampus (Ai, Aii), and the 14 months old hippocampus (Bi, Bii), in  
323 controls (Ai, Bi) and APP/PS1 (Aii, Bii). Scale bars = 20 $\mu$ m. (Aiii-Biii) Box-Whisker plots of the  
324 total area of OPC process domains. Data are Mean  $\pm$  SEM, \*\*\* $p$ <0.001, ANOVA, followed by  
325 Tukey's post hoc test,  $n$ =10 cells for WT-9mo and APP-9mo,  $n$ =13 cells for WT-14mo and  $n$ =17  
326 cells for APP-14mo, from 3 animals in each group.

327 **Figure 4. OPC morphological changes in the CA1 of the 14 months old APP/PS1 mouse model**  
 328 **compared to an aged-matched control.** Data were generated by NeuroLucida 360 analysis of cells.  
 329 Box-whisker plots of (A) cell body area, (B) cell body volume, (C) process volume, (D) total cell  
 330 volume, (E) cell complexity, (F) ramification index. Data expressed as Mean±SEM. ANOVA,  
 331 followed by Tukey's post hoc test, \* $p \leq 0.05$ , \*\* $p \leq 0.01$ ;  $n = 9$  cells from 3 animals in each group.

332 **Figure 5. Sholl analysis of age-related changes in OPC morphology in APP/PS1 and age-**  
 333 **matched controls.** (A) 3D morphology of NG2 immunolabelled OPC in the CA1 area of the  
 334 hippocampus (generated using isosurface rendering with Volocity software, PerkinElmer),  
 335 illustrating Sholl shells (concentric circles, 5  $\mu\text{m}$  apart, with the cell body in the middle), and the  
 336 morphological parameters measured; the points of process branching are termed nodes (blue dots),  
 337 the points where the processes intersect the Sholl shells are termed intersections (yellow dots), the  
 338 number of process terminals or end points, and the process branch order, with 1<sup>st</sup> order closest to the  
 339 cell body (adapted from Sholl 1953 and Rietveld et al. 2015). (B-E) Graphs comparing OPC  
 340 morphological parameters in AAP/PS1 mice aged 9 months (-●-) and 14 months (-■-), together with  
 341 age-matched controls (insets); two-way ANOVA followed by Sidak's multiple comparisons test.  
 342 \* $p < 0.05$ , \*\* $p < 0.01$ , \*\*\* $p < 0.001$ ,  $p < 0.0001$ .  $n = 9$  cells from 3 animals in each group.

343

#### 344 References

345

- 346 ABRAHAM, H., VINCZE, A., JEWGENOW, I., VESZPREMI, B., KRAVJAK, A., GOMORI, E. & SERESS, L.  
 347 2010. Myelination in the human hippocampal formation from midgestation to adulthood. *Int*  
 348 *J Dev Neurosci*, 28, 401-10.
- 349 BARTZOKIS, G. 2011. Alzheimer's disease as homeostatic responses to age-related myelin breakdown.  
 350 *Neurobiology of aging*, 32, 1341-1371.
- 351 BERGLES, D. E., ROBERTS, J. D., SOMOGYI, P. & JAHR, C. E. 2000. Glutamatergic synapses on  
 352 oligodendrocyte precursor cells in the hippocampus. *Nature*, 405, 187-91.
- 353 BODA, E., DI MARIA, S., ROSA, P., TAYLOR, V., ABBRACCHIO, M. P. & BUFFO, A. 2014. Early phenotypic  
 354 asymmetry of sister oligodendrocyte progenitor cells after mitosis and its modulation by aging  
 355 and extrinsic factors. *Glia*.
- 356 BORCHELT, D. R., RATOVITSKI, T., VAN LARE, J., LEE, M. K., GONZALES, V., JENKINS, N. A., COPELAND,  
 357 N. G., PRICE, D. L. & SISODIA, S. S. 1997. Accelerated amyloid deposition in the brains of  
 358 transgenic mice coexpressing mutant presenilin 1 and amyloid precursor proteins. *Neuron*,  
 359 19, 939-45.
- 360 BRAAK, H. & BRAAK, E. 1991. Neuropathological staging of Alzheimer-related changes. *Acta*  
 361 *Neuropathologica*, 82, 239-259.
- 362 BRICKMAN, A. M., ZAHODNE, L. B., GUZMAN, V. A., NARKHEDE, A., MEIER, I. B., GRIFFITH, E. Y.,  
 363 PROVENZANO, F. A., SCHUPF, N., MANLY, J. J., STERN, Y., LUCHSINGER, J. A. & MAYEUX, R.

- 364 2015. Reconsidering harbingers of dementia: progression of parietal lobe white matter  
365 hyperintensities predicts Alzheimer's disease incidence. *Neurobiol Aging*, 36, 27-32.
- 366 BUTT, A. M., DE LA ROCHA, I. C. & RIVERA, A. 2019a. Oligodendroglial Cells in Alzheimer's Disease.  
367 *Adv Exp Med Biol*, 1175, 325-333.
- 368 BUTT, A. M., HAMILTON, N., HUBBARD, P., PUGH, M. & IBRAHIM, M. 2005. Synantocytes: the fifth  
369 element. *Journal of Anatomy*, 207, 695-706.
- 370 BUTT, A. M., KIFF, J., HUBBARD, P. & BERRY, M. 2002. Synantocytes: New functions for novel NG2  
371 expressing glia. *Journal of Neurocytology*, 31, 551 ppl=-565.
- 372 BUTT, A. M., PAPANIKOLAOU, M. & RIVERA, A. 2019b. Physiology of Oligodendroglia. *Adv Exp Med  
373 Biol*, 1175, 117-128.
- 374 CHACON-DE-LA-ROCHA, I., FRYATT, G. L., RIVERA, A. D., RESTANI, L., CALEO, M., RAINETEAU, O.,  
375 GOMEZ-NICOLA, D. & BUTT, A. M. 2020. Synaptic silencing affects the density and complexity  
376 of oligodendrocyte precursor cells in the adult mouse hippocampus. *bioRxiv*,  
377 2020.09.23.309682.
- 378 CHAO, F.-L., ZHANG, L., ZHANG, Y., ZHOU, C.-N., JIANG, L., XIAO, Q., LUO, Y.-M., LV, F.-L., HE, Q. &  
379 TANG, Y. 2018. Running exercise protects against myelin breakdown in the absence of  
380 neurogenesis in the hippocampus of AD mice. *Brain Research*, 1684, 50-59.
- 381 CHORGHAY, Z., KARADOTTIR, R. T. & RUTHAZER, E. S. 2018. White Matter Plasticity Keeps the Brain  
382 in Tune: Axons Conduct While Glia Wrap. *Front Cell Neurosci*, 12, 428.
- 383 DESAI, M. K., SUDOL, K. L., JANELSINS, M. C., MASTRANGELO, M. A., FRAZER, M. E. & BOWERS, W. J.  
384 2009. Triple-transgenic Alzheimer's disease mice exhibit region-specific abnormalities in brain  
385 myelination patterns prior to appearance of amyloid and tau pathology. *Glia*, 57, 54-65.
- 386 DIMOU, L., SIMON, C., KIRCHHOFF, F., TAKEBAYASHI, H. & GÖTZ, M. 2008. Progeny of Olig2-  
387 expressing progenitors in the gray and white matter of the adult mouse cerebral cortex. *J  
388 Neurosci*, 28, 10434-42.
- 389 DONG, Y. X., ZHANG, H. Y., LI, H. Y., LIU, P. H., SUI, Y. & SUN, X. H. 2018. Association between  
390 Alzheimer's disease pathogenesis and early demyelination and oligodendrocyte dysfunction.  
391 *Neural Regen Res*, 13, 908-914.
- 392 FOSTER, A. Y., BUJALKA, H. & EMERY, B. 2019. Axoglial interactions in myelin plasticity: Evaluating the  
393 relationship between neuronal activity and oligodendrocyte dynamics. *Glia*.
- 394 GENGLER, S., HAMILTON, A. & HÖLSCHER, C. 2010. Synaptic plasticity in the hippocampus of a  
395 APP/PS1 mouse model of Alzheimer's disease is impaired in old but not young mice. *PLoS One*,  
396 5, e9764.
- 397 GIBSON, E. M., PURGER, D., MOUNT, C. W., GOLDSTEIN, A. K., LIN, G. L., WOOD, L. S., INEMA, I.,  
398 MILLER, S. E., BIERI, G., ZUCHERO, J. B., BARRES, B. A., WOO, P. J., VOGEL, H. & MONJE, M.  
399 2014. Neuronal activity promotes oligodendrogenesis and adaptive myelination in the  
400 mammalian brain. *Science*, 344, 1252304.
- 401 HAMILTON, N., VAYRO, S., WIGLEY, R. & BUTT, A. M. 2010. Axons and astrocytes release ATP and  
402 glutamate to evoke calcium signals in NG2-glia. *Glia*, 58, 66-79.

- 403 HILL, R. A., LI, A. M. & GRUTZENDLER, J. 2018. Lifelong cortical myelin plasticity and age-related  
404 degeneration in the live mammalian brain. *Nat Neurosci*, 21, 683-695.
- 405 HUGHES, E. G., ORTHMANN-MURPHY, J. L., LANGSETH, A. J. & BERGLES, D. E. 2018. Myelin remodeling  
406 through experience-dependent oligodendrogenesis in the adult somatosensory cortex. *Nat*  
407 *Neurosci*, 21, 696-706.
- 408 IHARA, M., POLVIKOSKI, T. M., HALL, R., SLADE, J. Y., PERRY, R. H., OAKLEY, A. E., ENGLUND, E.,  
409 O'BRIEN, J. T., INCE, P. G. & KALARIA, R. N. 2010. Quantification of myelin loss in frontal lobe  
410 white matter in vascular dementia, Alzheimer's disease, and dementia with Lewy bodies. *Acta*  
411 *Neuropathol*, 119, 579-89.
- 412 JIN, X., RIEW, T.-R., KIM, H. L., CHOI, J.-H. & LEE, M.-Y. 2018. Morphological characterization of NG2  
413 glia and their association with neuroglial cells in the 3-nitropropionic acid-lesioned striatum  
414 of rat. *Scientific reports*, 8, 5942-5942.
- 415 KANG, S. H., FUKAYA, M., YANG, J. K., ROTHSTEIN, J. D. & BERGLES, D. E. 2010. NG2+ CNS glial  
416 progenitors remain committed to the oligodendrocyte lineage in postnatal life and following  
417 neurodegeneration. *Neuron*, 68, 668-81.
- 418 LI, W., TANG, Y., FAN, Z., MENG, Y., YANG, G., LUO, J. & KE, Z. J. 2013. Autophagy is involved in  
419 oligodendroglial precursor-mediated clearance of amyloid peptide. *Mol Neurodegener*, 8, 27.
- 420 MCKENZIE, I. A., OHAYON, D., LI, H., DE FARIA, J. P., EMERY, B., TOHYAMA, K. & RICHARDSON, W. D.  
421 2014. Motor skill learning requires active central myelination. *Science*, 346, 318-22.
- 422 MITEW, S., KIRKCALDIE, M. T., HALLIDAY, G. M., SHEPHERD, C. E., VICKERS, J. C. & DICKSON, T. C. 2010.  
423 Focal demyelination in Alzheimer's disease and transgenic mouse models. *Acta Neuropathol*,  
424 119, 567-77.
- 425 NIELSEN, H. M., EK, D., AVDIC, U., ORBJÖRN, C., HANSSON, O., NETHERLANDS BRAIN, B., VEERHUIS,  
426 R., ROZEMULLER, A. J., BRUN, A., MINTHON, L. & WENNSTRÖM, M. 2013a. NG2 cells, a new  
427 trail for Alzheimer's disease mechanisms? *Acta neuropathologica communications*, 1, 7-7.
- 428 NIELSEN, H. M., EK, D., AVDIC, U., ORBJÖRN, C., HANSSON, O., VEERHUIS, R., ROZEMULLER, A. J.,  
429 BRUN, A., MINTHON, L., WENNSTRÖM, M. & BANK, N. B. 2013b. NG2 cells, a new trail for  
430 Alzheimer's disease mechanisms? *Acta Neuropathol Commun*, 1, 7.
- 431 NISHIYAMA, A., BOSHANS, L., GONCALVES, C. M., WEGRZYN, J. & PATEL, K. D. 2016. Lineage, fate, and  
432 fate potential of NG2-glia. *Brain Res*, 1638, 116-128.
- 433 ONG, W. Y. & LEVINE, J. M. 1999. A light and electron microscopic study of NG2 chondroitin sulfate  
434 proteoglycan-positive oligodendrocyte precursor cells in the normal and kainate-lesioned rat  
435 hippocampus. *Neuroscience*, 92, 83-95.
- 436 ORTIZ, F. C., HABERMACHER, C., GRACIARENA, M., HOURY, P. Y., NISHIYAMA, A., OUMESMAR, B. N.  
437 & ANGULO, M. C. 2019. Neuronal activity in vivo enhances functional myelin repair. *JCI Insight*,  
438 5.
- 439 OTA, M., SATO, N., KIMURA, Y., SHIGEMOTO, Y., KUNUGI, H. & MATSUDA, H. 2019. Changes of Myelin  
440 Organization in Patients with Alzheimer's Disease Shown by q-Space Myelin Map Imaging.  
441 *Dementia and Geriatric Cognitive Disorders Extra*, 9, 24-33.

- 442 PILLAI, A. G., DE JONG, D., KANATSOU, S., KRUGERS, H., KNAPMAN, A., HEINZMANN, J.-M.,  
443 HOLSBOER, F., LANDGRAF, R., JOËLS, M. & TOUMA, C. 2012. Dendritic Morphology of  
444 Hippocampal and Amygdalar Neurons in Adolescent Mice Is Resilient to Genetic Differences  
445 in Stress Reactivity. *PLOS ONE*, 7, e38971.
- 446 PSACHOULIA, K., JAMEN, F., YOUNG, K. M. & RICHARDSON, W. D. 2009. Cell cycle dynamics of NG2  
447 cells in the postnatal and ageing brain. *Neuron Glia Biol*, 5, 57-67.
- 448 RIVERA, A., VANZULI, I., ARELLANO, J. J. & BUTT, A. 2016. Decreased Regenerative Capacity of  
449 Oligodendrocyte Progenitor Cells (NG2-Glia) in the Ageing Brain: A Vicious Cycle of Synaptic  
450 Dysfunction, Myelin Loss and Neuronal Disruption? *Curr Alzheimer Res*, 13, 413-8.
- 451 RIVERS, L. E., YOUNG, K. M., RIZZI, M., JAMEN, F., PSACHOULIA, K., WADE, A., KESSARIS, N. &  
452 RICHARDSON, W. D. 2008. PDGFRA/NG2 glia generate myelinating oligodendrocytes and  
453 piriform projection neurons in adult mice. *Nat Neurosci*, 11, 1392-401.
- 454 RODRÍGUEZ, J. J., BUTT, A. M., GARDENAL, E., PARPURA, V. & VERKHRATSKY, A. 2016. Complex and  
455 differential glial responses in Alzheimer's disease and ageing. *Curr Alzheimer Res*, 13, 343-58.
- 456 SHU, X., QIN, Y. Y., ZHANG, S., JIANG, J. J., ZHANG, Y., ZHAO, L. Y., SHAN, D. & ZHU, W. Z. 2013. Voxel-  
457 based diffusion tensor imaging of an APP/PS1 mouse model of Alzheimer's disease. *Mol*  
458 *Neurobiol*, 48, 78-83.
- 459 SJÖBECK, M. & ENGLUND, E. 2003. Glial levels determine severity of white matter disease in  
460 Alzheimer's disease: a neuropathological study of glial changes. *Neuropathology and Applied*  
461 *Neurobiology*, 29, 159-169.
- 462 STEADMAN, P. E., XIA, F., AHMED, M., MOCLE, A. J., PENNING, A. R. A., GERAGHTY, A. C., STEENLAND,  
463 H. W., MONJE, M., JOSSELYN, S. A. & FRANKLAND, P. W. 2020. Disruption of  
464 Oligodendrogenesis Impairs Memory Consolidation in Adult Mice. *Neuron*, 105, 150-164.e6.
- 465 VANZULLI, I., PAPANIKOLAOU, M., DE LA ROCHA, I. C., PIEROPAN, F., RIVERA, A. D., GOMEZ-NICOLA,  
466 D., VERKHRATSKY, A., RODRÍGUEZ, J. J. & BUTT, A. M. 2020. Disruption of oligodendrocyte  
467 progenitor cells is an early sign of pathology in the triple transgenic mouse model of  
468 Alzheimer's disease. *Neurobiology of Aging*.
- 469 VIGANÒ, F., SCHNEIDER, S., CIMINO, M., BONFANTI, E., GELOSA, P., SIRONI, L., ABBRACCHIO, M. P. &  
470 DIMOU, L. 2016. GPR17 expressing NG2-Glia: Oligodendrocyte progenitors serving as a  
471 reserve pool after injury. *Glia*, 64, 287-99.
- 472 WAKE, H., LEE, P. R. & FIELDS, R. D. 2011. Control of local protein synthesis and initial events in  
473 myelination by action potentials. *Science*, 333, 1647-51.
- 474 WILLIAMSON, J. M. & LYONS, D. A. 2018. Myelin Dynamics Throughout Life: An Ever-Changing  
475 Landscape? *Front Cell Neurosci*, 12, 424.
- 476 WU, Y., MA, Y., LIU, Z., GENG, Q., CHEN, Z. & ZHANG, Y. 2017. Alterations of myelin morphology and  
477 oligodendrocyte development in early stage of Alzheimer's disease mouse model. *Neurosci*  
478 *Lett*, 642, 102-106.
- 479 XIAO, L., OHAYON, D., MCKENZIE, I. A., SINCLAIR-WILSON, A., WRIGHT, J. L., FUDGE, A. D., EMERY, B.,  
480 LI, H. & RICHARDSON, W. D. 2016. Rapid production of new oligodendrocytes is required in  
481 the earliest stages of motor-skill learning. *Nat Neurosci*, 19, 1210-7.

482 YOUNG, K. M., PSACHOULIA, K., TRIPATHI, R. B., DUNN, S.-J., COSSELL, L., ATTWELL, D., TOHYAMA, K.  
 483 & RICHARDSON, W. D. 2013. Oligodendrocyte dynamics in the healthy adult CNS: evidence for  
 484 myelin remodeling. *Neuron*, 77, 873-885.

485 ZHANG, P., KISHIMOTO, Y., GRAMMATIKAKIS, I., GOTTIMUKKALA, K., CUTLER, R. G., ZHANG, S.,  
 486 ABDELMOHSEN, K., BOHR, V. A., MISRA SEN, J., GOROSPE, M. & MATTSON, M. P. 2019.  
 487 Senolytic therapy alleviates A $\beta$ -associated oligodendrocyte progenitor cell senescence and  
 488 cognitive deficits in an Alzheimer's disease model. *Nat Neurosci*, 22, 719-728.

489 ZHU, X., HILL, R. A. & NISHIYAMA, A. 2008. NG2 cells generate oligodendrocytes and gray matter  
 490 astrocytes in the spinal cord. *Neuron Glia Biol*, 4, 19-26.

491

492

In review

Figure 1.JPEG

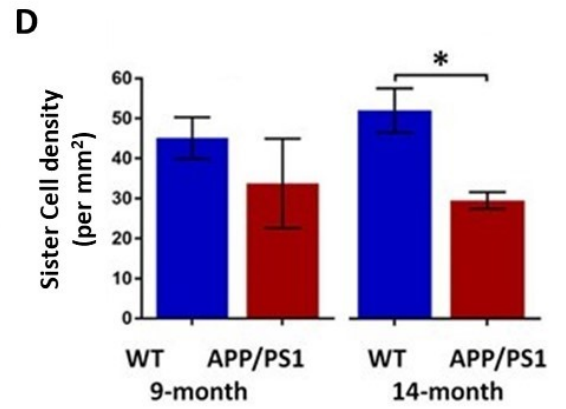
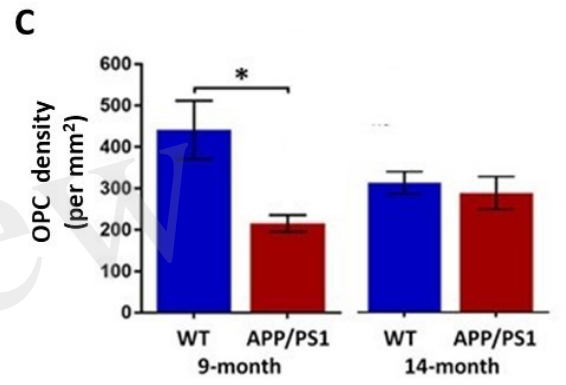
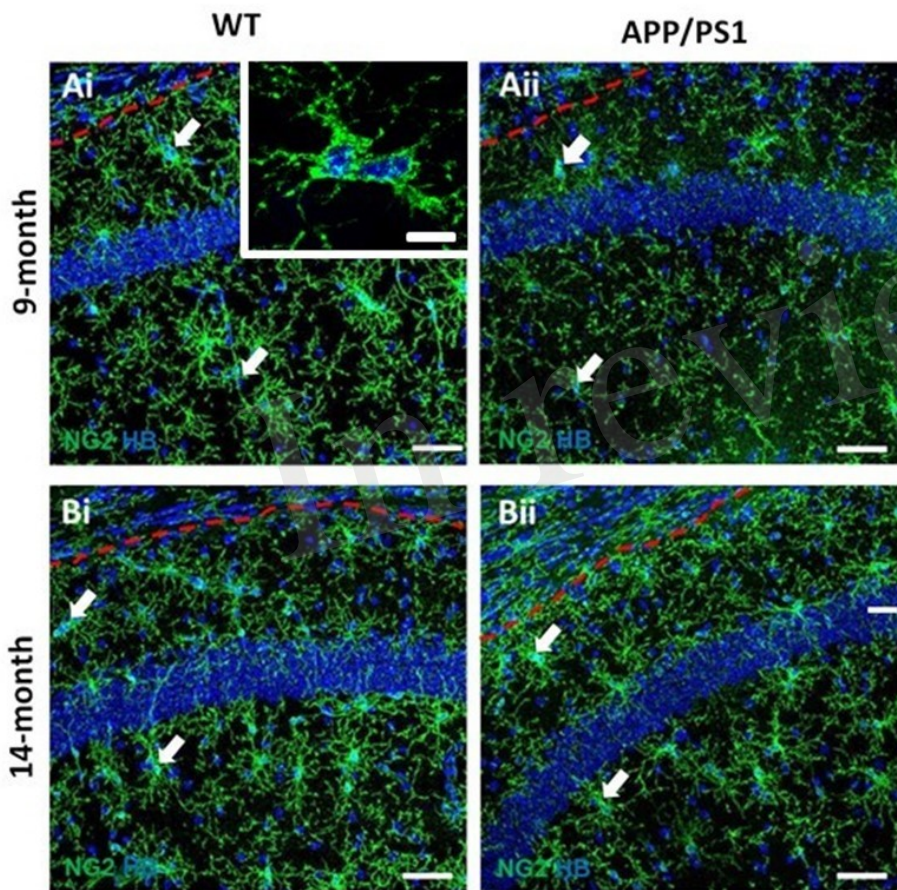


Figure 2.JPEG

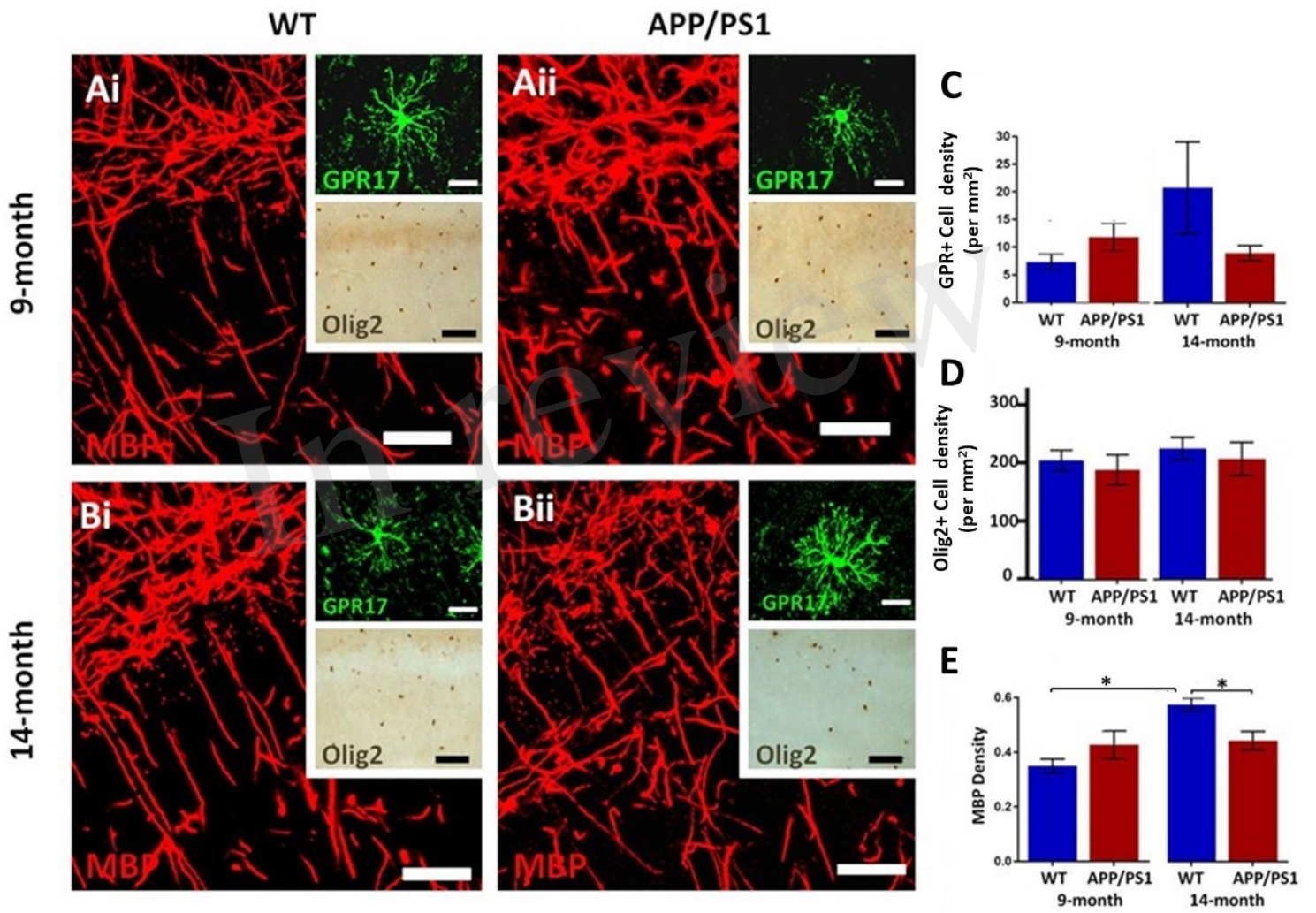
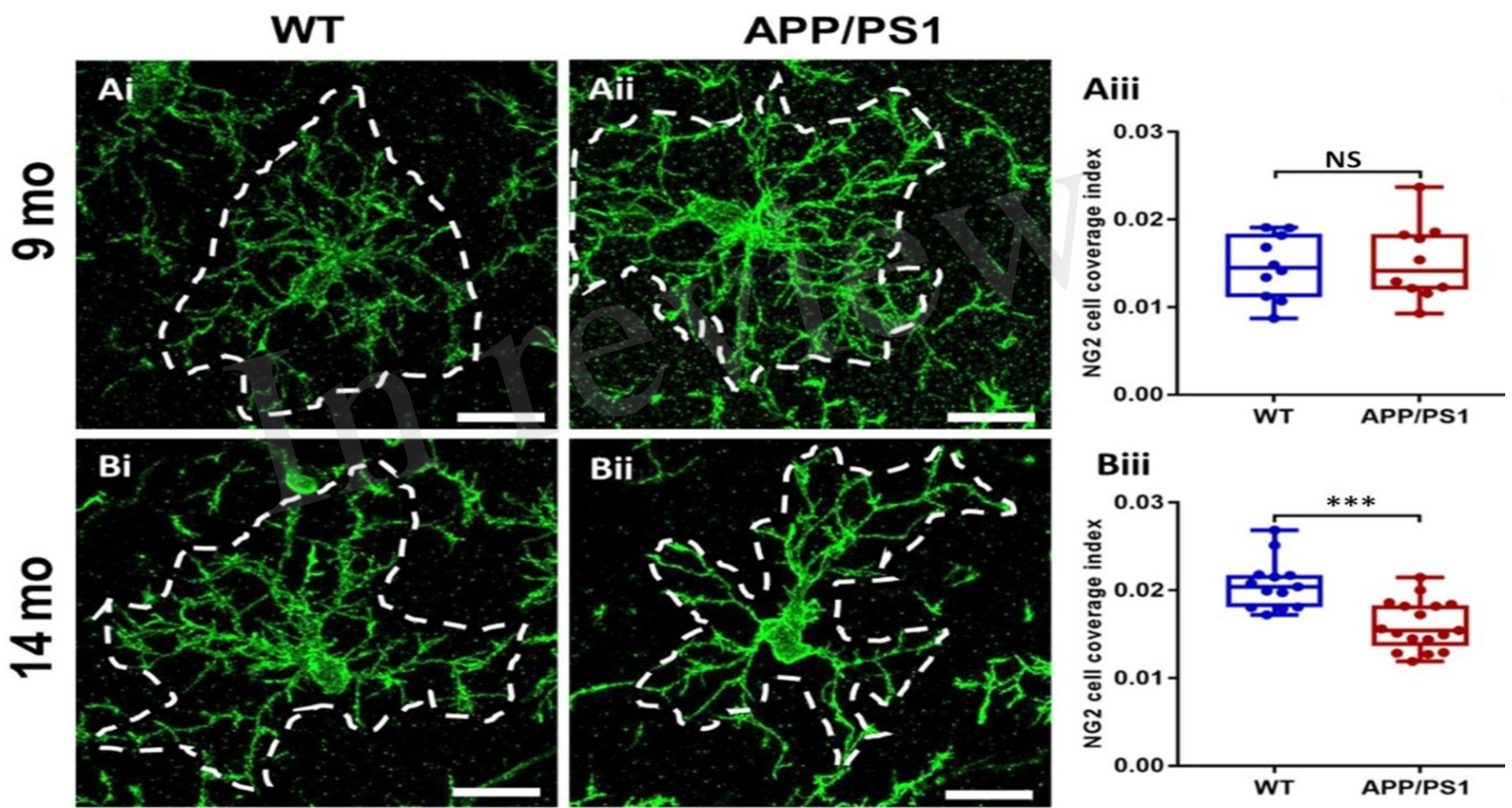


Figure 3.JPEG



WT

Figure 4.JPEG

APP/PS1

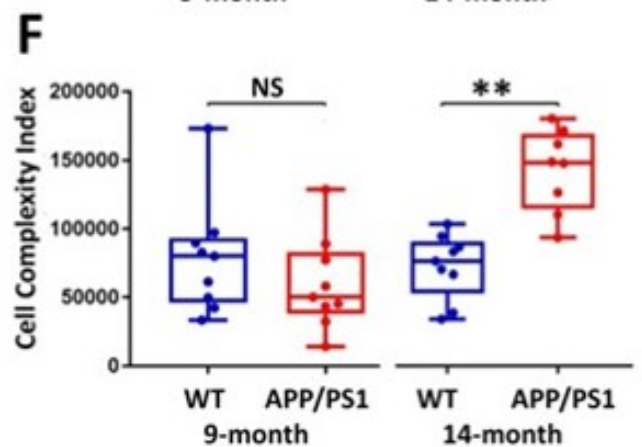
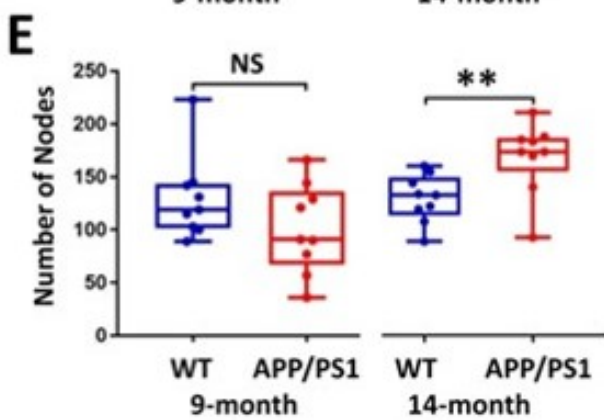
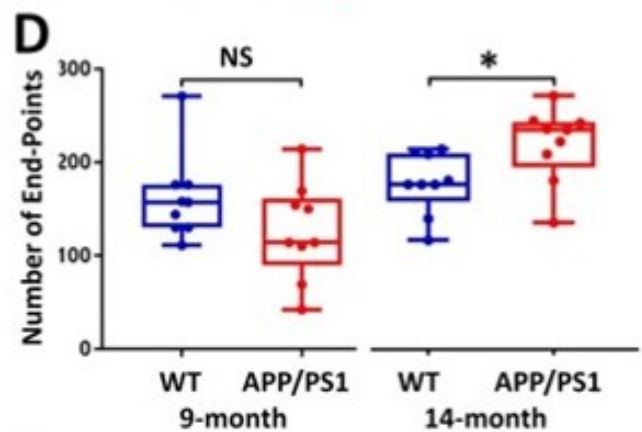
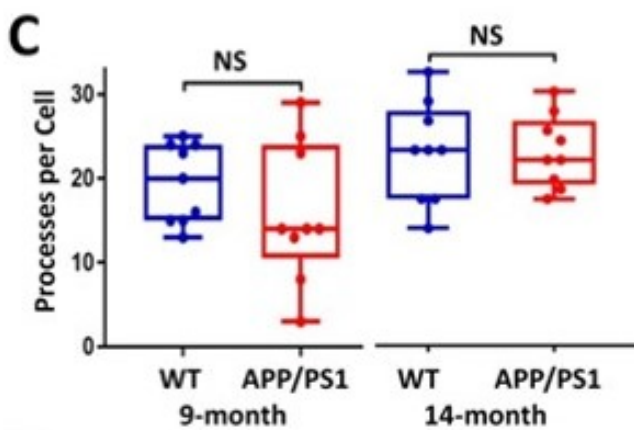
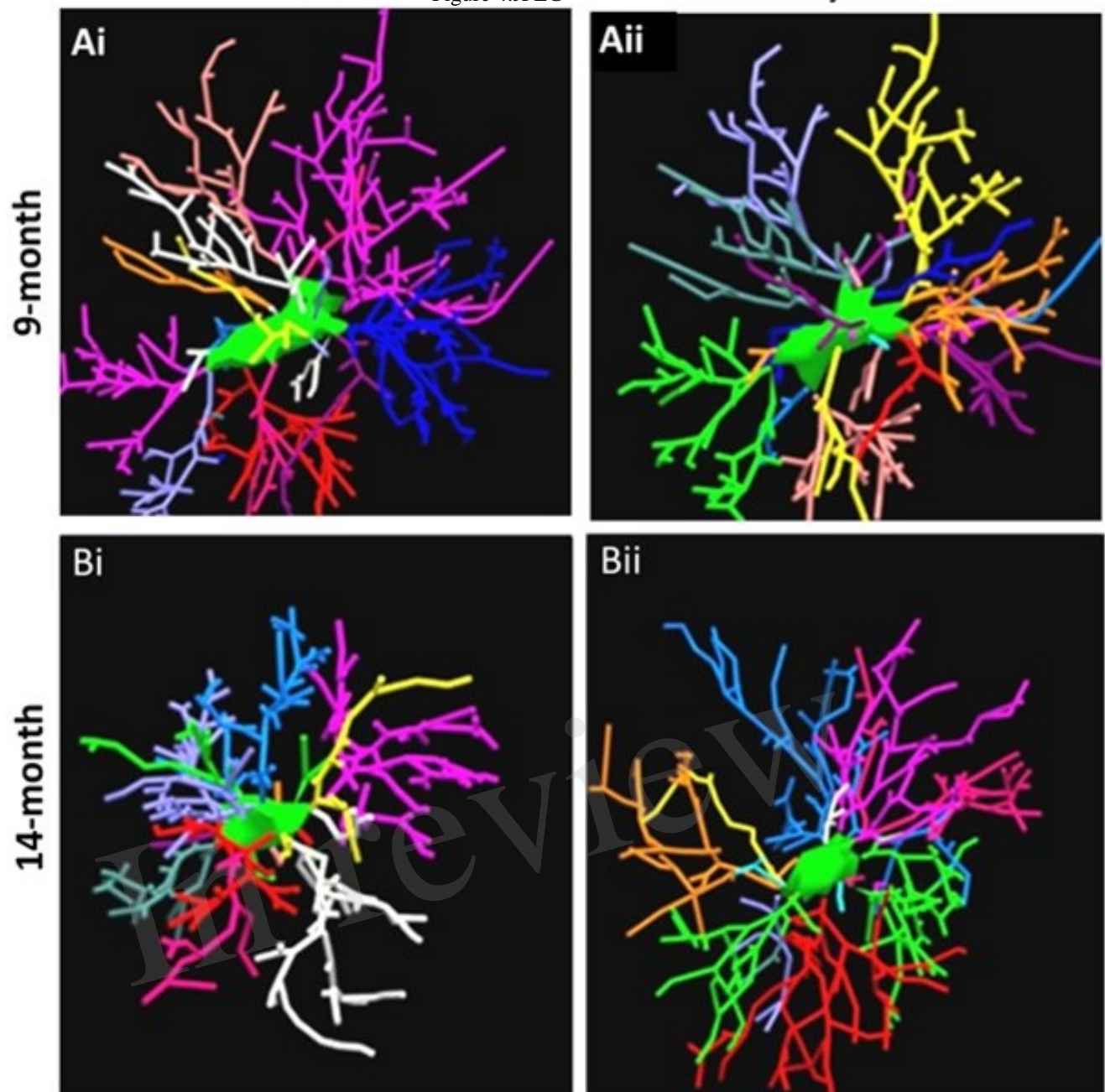


Figure 5.JPEG

In review

